Atmospheric Environment 141 (2016) 422–429

Contents lists available at ScienceDirect

Atmospheric Environment

journal homepage: www.elsevier.com/locate/atmosenv

Uncertainty of modelled urban peak O_3 concentrations and its sensitivity to input data perturbations based on the Monte Carlo analysis

Andrea L. Pineda Rojas [a, *], Laura E. Venegas [b], Nicolás A. Mazzeo [b]

[a] Centro de Investigaciones del Mar y la Atmósfera (CIMA/CONICET-UBA), DCAO/FCEN, UMI-IFAECI/CNRS, Ciudad Universitaria, Pabellón II, Piso 2. 1428, Buenos Aires, Argentina
[b] Department of Chemical Engineering, Avellaneda Regional Faculty, National Technological University, CONICET, Av. Ramón Franco 5050, 1874, Avellaneda, Buenos Aires, Argentina

HIGHLIGHTS

- Modelled peak O_3 concentrations in the MABA during the summer are analysed.
- Larger uncertainty levels are associated with larger ozone concentrations.
- The uncertainty contributions from the model input variables vary spatially.
- That of the regional background O_3 concentration dominates at all analysed receptors.
- Model sensitivity responses have similarities with those obtained with complex models.

ARTICLE INFO

Article history:
Received 15 January 2016
Received in revised form
23 June 2016
Accepted 7 July 2016
Available online 9 July 2016

Keywords:
Air quality
Model uncertainty
Sensitivity
Ozone
Monte Carlo analysis

ABSTRACT

A simple urban air quality model [MODelo de Dispersión Atmosférica Ubana – Generic Reaction Set (DAUMOD-GRS)] was recently developed. One-hour peak O_3 concentrations in the Metropolitan Area of Buenos Aires (MABA) during the summer estimated with the DAUMOD-GRS model have shown values lower than 20 ppb (the regional background concentration) in the urban area and levels greater than 40 ppb in its surroundings. Due to the lack of measurements outside the MABA, these relatively high ozone modelled concentrations constitute the only estimate for the area. In this work, a methodology based on the Monte Carlo analysis is implemented to evaluate the uncertainty in these modelled concentrations associated to possible errors of the model input data. Results show that the larger 1-h peak O_3 levels in the MABA during the summer present larger uncertainties (up to 47 ppb). On the other hand, multiple linear regression analysis is applied at selected receptors in order to identify the variables explaining most of the obtained variance. Although their relative contributions vary spatially, the uncertainty of the regional background O_3 concentration dominates at all the analysed receptors (34.4–97.6%), indicating that their estimations could be improved to enhance the ability of the model to simulate peak O_3 concentrations in the MABA.

1. Introduction

Ozone (O_3) is known among the air pollutants to have great potential to cause adverse effects on human health and the environment (WHO, 2014). Ground-level O_3 concentrations are increasing in many cities of the world and their surroundings due to changing emissions of nitrogen oxides ($NO_x = NO + NO_2$) and volatile organic compounds (VOCs) from human activities and other environmental factors such as temperature (e.g., Lee et al., 2014; Paoletti et al., 2014; Wang et al., 2012). The typical horizontal distribution of ozone concentration shows a relative minimum in the urban areas (due to O_3 titration by NO in zones of large NO_x emissions) and a maximum several kilometres downwind of cities (as a consequence of an "optimal" VOCs/NO_x concentration ratio for ozone formation (Calfapietra et al., 2013)). In order to assure that its levels remain relatively low, the spatio-temporal distribution of

* Corresponding author.
E-mail address: pineda@cima.fcen.uba.ar (A.L. Pineda Rojas).

http://dx.doi.org/10.1016/j.atmosenv.2016.07.020
1352-2310/

ozone concentrations in urban areas should be evaluated. In places where this is not satisfied, pollution mitigation actions must be taken to reduce ozone concentrations. This type of air quality assessment is achieved through the combined use of observations providing precise information at specific monitoring sites and air quality models which allow the estimation of the concentration distribution in a given area. Since these models provide a link between emissions, meteorology and concentrations, they are also widely used by researchers to study a number of air quality issues such as process analysis (e.g., Wang et al., 2012), source apportionment (e.g., Strong et al., 2013) and the possible impact of climate change on O_3 levels (e.g., Athanassiadou et al., 2010), to name a few.

When modelled concentrations are used either for policy decision making or for scientific purposes, a measure of their reliability can be required. This is given by the model performance evaluation which involves different steps of varying complexity depending on the model type and specific purpose. Three common fundamental aspects of the performance evaluation of an air quality model are: the scientific evaluation, the statistical evaluation and the probabilistic evaluation (e.g., Chang and Hanna, 2005; Derwent et al., 2010). The former examines model algorithms and model assumptions in detail. The statistical evaluation refers to the comparison between modelled and observed concentrations, and plays an essential role since it provides a measure of the "total error" of the model. Finally, the probabilistic sensitivity/uncertainty evaluation aims to capture the uncertainty in model results introduced by variabilities of a specific parameter, variable, parameterisation, or a combination of them, etc. In air quality models applications, the uncertainty of the model input data is considered to be the dominant source of error (Russell and Dennis, 2000). Uncertainty and sensitivity analysis offers a tool through which the uncertainty of modelled pollutant concentrations associated to input data uncertainties can be evaluated. This is critical for policy decision makers since air quality management must be based on a range of probable results rather than on a single value whose occurrence is subject to error. On the other hand, a good understanding of the key variables associated with model output uncertainties is fundamental. This allows modellers and scientists to gain insight into model strengths and weaknesses, as well as into the variables or parameters whose estimations should be improved in order to enhance model capabilities. There are different methodologies available throughout the literature to apply uncertainty and sensitivity analysis with air quality models (see Borrego et al., 2008; Refsgaard et al., 2007), where the Monte Carlo (MC) analysis combined with multiple linear regression (MLR) analysis is one of the most widely used methods to study the uncertainty of modelled pollutant concentrations (e.g., Bergin et al., 1999; Hanna et al., 1998, 2007; Moore and Londergan, 2001; Rodriguez et al., 2007; Tang et al., 2010). Other applications of the Monte Carlo analysis include the uncertainty assessment of the impact of different pollution mitigation strategies on peak O_3 levels (e.g., Derwent and Murrells, 2013) and the use of different sets of observations to estimate representative average pollutant concentrations (e.g., Tan et al., 2014).

The DAUMOD-GRS (MODelo de Dispersión Atmosférica Urbana – Generic Reaction Set) model (Pineda Rojas and Venegas, 2013a) is a simple atmospheric dispersion model that allows estimation of ground-level O_3 concentrations resulting from area source emissions of NO_x and VOCs in urban areas. It is based on the bidimensional equation of diffusion and employs a simplified photochemical scheme of the NO_x-VOCs-O_3 interactions. The model has been statistically evaluated using observations of nitrogen dioxide and ozone concentrations from twenty monitoring sites of the Metropolitan Area of Buenos Aires (MABA), Argentina, and has shown an acceptable performance (Pineda Rojas and Venegas, 2013b; Pineda Rojas, 2014). A series of features of the MABA (3830 km^2, ~13 million inhabitants), such as its flat terrain location or that it is surrounded by non-urban areas, support the use of simple models. The aim of the present work is to perform a probabilistic evaluation to analyse the uncertainty in modelled O_3 concentrations in the MABA associated to possible errors of the DAUMOD-GRS input variables. It is worth noting that previously simulated 1-h peak O_3 levels in the region during summer for the first time (Pineda Rojas and Venegas, 2013b) were found to be below the air quality standard for the region (120 ppb); however, values above 40 ppb [i.e., the threshold used in other parts of the world to protect vegetation (Paoletti and Manning, 2007)] were simulated for the surroundings of the MABA. Since there are no measurements outside the MABA to compare these potentially high modelled O_3 concentrations with, a probabilistic evaluation of these concentrations becomes critical. In this work, we implement a methodology based on the MC and MLR techniques to perform an uncertainty and sensitivity analysis of the DAUMOD-GRS model. The objectives of the present paper are 1) to evaluate the uncertainty of modelled 1-h peak O_3 concentrations at each receptor in the MABA region during the summer associated to uncertainties in the input variables, and 2) to determine the subset of variables explaining most of the obtained variance.

2. Methodology

The Monte Carlo (MC) analysis consists of performing a relatively large number of simulations (called MC runs) using different combinations of alternative values for model input variables, which are randomly obtained from their probability density functions and uncertainty ranges. As a result, a set of probable values of the modelled pollutant concentration is obtained, from which a number of statistics can be computed. The main advantages of the MC analysis are its general applicability and the relatively few assumptions that it needs. Common drawbacks are that probability density functions and uncertainty ranges of the input variables are often unknown, and that the method generates a huge amount of data that is usually difficult to analyse. The multiple linear regression (MLR) analysis offers a way of characterising the input-output transformations (i.e., the relationship between the perturbed input variables and the pollutant concentrations obtained from the MC runs) so that the uncertainty contribution of each input variable to the total uncertainty of the modelled concentration can be easily estimated. Here, the MC analysis is implemented to evaluate the uncertainty of modelled 1-h peak O_3 concentrations at each receptor in the MABA during the summer (C_{max}) associated to possible errors in the input variables; while MLR analysis is performed to estimate their relative contributions. The implementation of these techniques with DAUMOD-GRS is based on their previous applications with other air quality models (Bergin et al., 1999; Hanna et al., 1998, 2007; Moore and Londergan, 2001; Rodriguez et al., 2007), with slight modifications as described in the following sections. Section 2.1 comments on the main features of the DAUMOD-GRS model. Section 2.2 describes the implementation of the Monte Carlo analysis with the DAUMOD-GRS model and Section 2.3 the application of the multiple linear regression analysis to estimate the contribution of the uncertainty of input variables to the modelled C_{max} uncertainty.

2.1. Model characteristics

The DAUMOD-GRS model couples the MODelo de DispersiónAtmosférica Urbana (DAUMOD) with the Generic Reaction Set (GRS). The DAUMOD model (Mazzeo and Venegas, 1991) is

based on the bidimensional diffusion equation and allows the estimation of baseline urban pollutant concentrations (i.e., concentrations that result from all urban emission sources at a given area). This model and successive versions have been used extensively to study several air quality issues in the MABA (e.g., Mazzeo and Venegas, 2008; Pineda Rojas and Venegas, 2009; Venegas and Mazzeo, 2006; Venegas et al., 2011). The GRS (Azzi et al., 1992) is a simplified photochemical scheme that simulates O_3 formation in the urban atmosphere with only seven reactions and which has been included in the algorithms of several air quality models (e.g., Kim et al., 2005; Hurley et al., 2005; Venkatram et al., 1994). A key input variable for the GRS is the initial O_3 concentration. In the DAUMOD-GRS model, this is given by the sum of the regional background O_3 level and the O_3 concentration remaining from the previous time step, computed at each receptor and time, and representing the "memory effect". A detailed description of the DAUMOD-GRS model can be found in Pineda Rojas and Venegas (2013a). The performance of the model to simulate hourly nitrogen dioxide and ozone concentrations at twenty monitoring sites in the MABA has been shown to be acceptable (Pineda Rojas, 2014). In particular, the comparison of modelled and observed daily 1-h maximum O_3 concentrations showed a normalised mean square error of 0.11, a fractional bias of −0.139 and a fraction of 0.86 of model results that fall within ±50% of the observed values (Pineda Rojas and Venegas, 2013b).

Based on the features of the two original models, the coupled model DAUMOD-GRS allows the estimation of O_3 concentrations resulting from urban area source emissions of NO_x and VOCs at high spatial and temporal resolutions (1 km^2, 1 h), long-term periods (e.g., 1 year), and from relatively little input data. These are its main advantages to apply the Monte Carlo analysis. In particular, its relatively low computational demand allows a large number of high resolution simulations for the whole metropolitan area and an entire summer period.

2.2. Implementation of the Monte Carlo analysis

The DAUMOD-GRS model input variables are: wind speed (U), wind direction (DIR), air temperature (T), sky cover (SC), atmospheric stability class (KST), total solar radiation (TSR), emission rate of nitrogen oxides (QNO_x), emission rate of volatile organic compounds (QVOC), and regional background ozone concentration ($[O_3]_r$). Due to the lack of available data, their probability density functions and uncertainty ranges are approximations based on data available from the literature (see Table 1). Note that these uncertainty values were obtained for other places and therefore may not be fully representative of the MABA conditions. For example, the $[O_3]_r$ uncertainty (30%) is taken from a study of Hanna et al. (1998) in which it was estimated for a larger domain. In the MABA, the uncertainty of this variable could be in fact greater than the value considered in this work due to upwind mesosescale source areas.

Table 1
Considered probability density functions (PDF) and uncertainty ranges of DAUMOD-GRS input variables (U: wind speed, DIR: wind direction, T: air temperature, SC: sky cover, KST: atmospheric stability class, TSR: total solar radiation, QNO_x: NO_x emission rate, QVOC: VOC emission rate, $[O_3]_r$: regional background O_3 concentration). N: normal distribution (uncertainty of 2σ), LN: log-normal distribution (uncertainty given in %).

Input variable	PDF	2σ/E(%)
U (%) [1]	LN	30
DIR (°) [1]	N	30
T (°C) [1]	N	3
SC (okta) [3]	N	1
KST [1]	N	1
TSR (%) [2]	LN	12.5
QNO_x (%) [1]	LN	40
QVOC (%) [1]	LN	80
$[O_3]_r$ (%) [1]	LN	30

Uncertainty ranges and PDF from Hanna et al., 1998[1], 2005[2], 2007.[3]

The Simple Random Sampling method (Moore and Londergan, 2001) is then applied to obtain N sets of uncertainty values for each of the nine input variables from their probability distributions. Apart from the input files for a standard run (base case), N additional files containing these sets of perturbations are generated. For simplicity, the randomly sampled perturbation of a given variable is assumed to be constant for the entire simulation period and modelling domain. In order to avoid an excessive generation of input files, a few code modifications are performed to let the model perturb the variables during the MC runs. On the other hand, correlations between input variables uncertainties are not considered. For normally and log-normally distributed variables (see Table 1) the sampled perturbation is added to and multiplied by its corresponding nominal value, respectively.

From the MC simulations, N alternative C_{max} values are obtained for each receptor, which are then used to evaluate the horizontal distribution of mean C_{max}. This technique is considered to give reliable results when N is sufficiently large so that the mean C_{max} values converge to those obtained from the base case run [C_{max}(BC)]. In this kind of Monte Carlo applications, a sample size of N = 100 is expected to capture the main aspects of the C_{max} uncertainty (Hanna et al., 2007). Once convergence is achieved, different statistical measures are usually calculated to quantify uncertainty [e.g., standard deviation (σ), coefficient of variation (COV = σx100/mean), interquartile range, 95% confidence interval]. In this work, the 95% confidence interval is considered as a measure of the C_{max} uncertainty.

The simulations are performed for an entire summer period (Dec, Jan, Feb), in a domain covering the MABA (3830 km^2) at a high spatial (1 km^2) and temporal (1 h) resolutions. The input data of the base case consists of hourly meteorological surface information and sounding data, measured at the Domestic and International airports respectively during the summer of 2007. Anthropogenic NO_x and VOCs area source emission data belong to the emissions inventory developed for the MABA (Venegas et al., 2011). On the other hand, the regional background O_3 concentration (the concentration that would exist if the MABA was not present) is considered to be a single constant value of 20 ppb based on results from two previous air quality monitoring campaigns carried out in the city of Buenos Aires (Bogo et al., 1999; Mazzeo et al., 2005). The regional background concentrations of other chemical species are considered to have "clean air" values based on the fact that the MABA is mainly surrounded by non-urban areas. The spatial distribution of C_{max}(BC) values estimated using the DAUMOD-GRS model in the MABA under these conditions was presented and discussed in Pineda Rojas and Venegas (2013b).

2.3. Application of multiple linear regression analysis

Multiple linear regression (MLR) analysis allows the model output variable (C_{max}) to be expressed as a linear function of the perturbed input variables (U, DIR, T, SC, KST, TSR, QNO_x, QVOC, $[O_3]_r$) using the results obtained from the MC runs. At a specific receptor, the pollutant concentration (normalized by the standard deviation) obtained in the simulation j can be expressed as:

$$C_j = \sum_{i=1}^{m} \beta_i x_{ij} + e_j \quad (1)$$

where β_i is the standardised multiple regression coefficient of the perturbed input variable x_i ($i = 1, \ldots, m$), x_{ij} is the normalised perturbed value of x_i in the simulation j ($j = 1, \ldots, N$), and e_j is the adjustment error. Coefficients β_i give a measure of the sensitivity of C to x_i, and they are commonly used to estimate the relative contributions of the input variables errors to the uncertainty of the modelled pollutant concentrations (e.g., Bergin et al., 1999; Hanna et al., 2007). Eq. (1) considers that only first order effects are significant, which is an acceptable assumption in the uncertainty and sensitivity analysis of air quality models. The major limitation of first-order sensitivities is that these describe the model response over a limited range of input parameters (Dunker et al., 2002) and do not account for nonlinear effects.

In order to make a good selection of the input-output variables to be analysed, it is important to emphasize that the purpose of using Eq. (1) is to quantify the effect of the input variables uncertainty on the C_{max} uncertainty. At a specific receptor, if C_{max} is found at different days in the different MC runs, then the variation of C_{max} (and hence its uncertainty) will depend not only on the perturbations of the input variables x_i but also on this change, in whose case erroneous conclusions could be inferred regarding the interpretation of the β_i values.

Most studies on the uncertainty and sensitivity analysis of peak O_3 concentrations are developed for episodes of a few days in which the C_{max} values obtained from different MC runs often occur at different hours but on the same day (e.g., Hanna et al., 2005), and therefore the change of conditions of the C_{max} occurrence is not expected to affect the results considerably. In this work, C_{max} refers to the 1-h peak O_3 concentration at each receptor in the MABA during the summer, and some preliminary tests have shown that at a given receptor it occurs at different days of the summer through the different MC simulations. To overcome this, the MLR analysis is performed considering the hourly O_3 concentration (C_h) modelled at the time of the occurrence of C_{max}(BC) as the output variable. This is done at selected receptors which are chosen aiming at covering different atmospheric and emission conditions associated to the occurrence of C_{max}(BC). The obtained standardised multiple regression coefficients (β_i) are then used to estimate the uncertainty contribution (UC_i) of the input variable x_i to the total uncertainty of C_h at each receptor.

3. Results

3.1. Uncertainty of C_{max} in the MABA

The DAUMOD-GRS model is applied to obtain N = 100 high resolution (1 km^2) distributions of the 1-h peak O_3 concentration at each receptor in the MABA during the summer (C_{max}). At each receptor, its mean, coefficient of variation, and 95% confidence interval are calculated.

Fig. 1 presents the spatial distribution of the mean C_{max} values (i.e., the average of C_{max} over the 100 MC simulation results). They vary between 15.3 and 50.9 ppb, with the lower values in the most urbanised zones (due to the highest NO_x emission rates). The mean C_{max} values obtained at each receptor of the MABA area are similar to those estimated previously for the base case (BC) run (Pineda Rojas and Venegas, 2013b), indicating that convergence is achieved with this number of simulations, as expected. Note that the highest mean C_{max} value of the modelling domain (50.9 ppb) is quite below the air quality standard for the MABA (120 ppb) which is expected based on the previous campaigns carried out in the city which showed relatively low (<50 ppb) O_3 hourly concentration levels (Bogo et al., 1999; Mazzeo et al., 2005).

The uncertainty of C_{max} (considered as the 95% confidence interval) varies between 9.3 and 47.0 ppb (see Fig. 2) and shows a

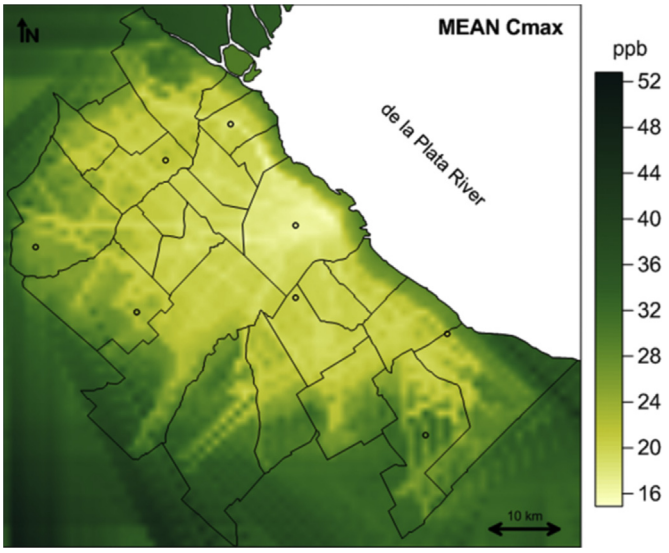

Fig. 1. Mean 1-h O_3 peak during the summer (C_{max}), calculated by averaging the results of 100 MC simulations.

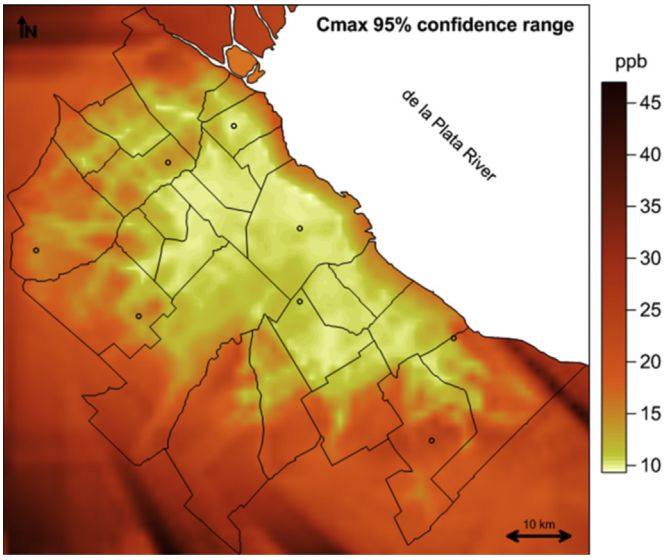

Fig. 2. 95% confidence interval of the 1-h peak O_3 concentration during the summer (C_{max}), obtained from the 100 MC simulations.

spatial pattern that indicates that the larger C_{max} values are associated to larger uncertainties. On the other hand, the horizontal distribution of the coefficient of variation of C_{max} (not shown) varies between 13.1 and 30.0%, which is within the range of results obtained in other modelling studies (Bergin et al., 1999; Hanna et al., 1998, 2005; Rodriguez et al., 2007; Russell and Dennis, 2000).

From Table 2, C_{max}(BC) values can occur under a wide range of conditions of wind speed (calm – 10.3 m/s) and wind direction (see Fig. 3), temperature (17.8–30.1 °C) and solar radiation (84.8–918.5 W/m^2). At receptors presenting relatively high emission rates (P1-P3), these values are found to be below the assumed regional background ozone level (20 ppb) and occur around midday hours. This means that, according to the model results, there is a net removal of ozone at these receptors (as expected). At receptors in the suburbs (P6-P8), C_{max} occurs at 7–8 h or 19 h during low wind conditions and it is found to be larger than 20 ppb,

Table 2
One-hour peak O_3 concentration at the selected receptors shown in Fig. 3 during the summer, obtained from the base case simulation [C_{max}(BC)]. Atmospheric conditions (U: wind speed, DIR: wind direction, T: air temperature, SC: sky cover, KST: atmospheric stability class, TSR: total solar radiation) and local emission conditions (QNO_x: NOx emission rate, QVOC: VOC emission rate) at the time of occurrence of C_{max}(BC) (M: month, D: day, H: hour).

Receptor	C_{max}(BC) (ppb)	M	D	H	U (m/s)	DIR	T (°C)	SC (Okta)	KST	TSR (W/m^2)	QNO_x (μg/m^{2}s)	QVOC (μg/m^{2}s)
P1	16.3	1	17	14	10.3	NW	30.1	0	3	878.6	10.12	2.71
P2	16.7	12	30	14	7.7	SE	30.1	0	2	918.5	4.05	2.69
P3	18.8	12	29	11	4.6	SW	26.2	2	2	854.0	2.41	1.29
P4	19.9	12	2	13	2.1	NE	27.3	2	1	915.9	1.11	0.59
P5	20.2	1	14	14	2.6	NNE	18.9	0	1	882.8	0.12	0.05
P6	23.1	1	15	7	1.0	WSW	17.8	0	5	155.8	0.11	0.04
P7	25.2	2	2	8	<1.0	NNW	25.1	0	5	319.4	0.09	0.04
P8	26.2	1	26	19	<1.0	ESE	25.1	2	3	84.8	0.00	0.00

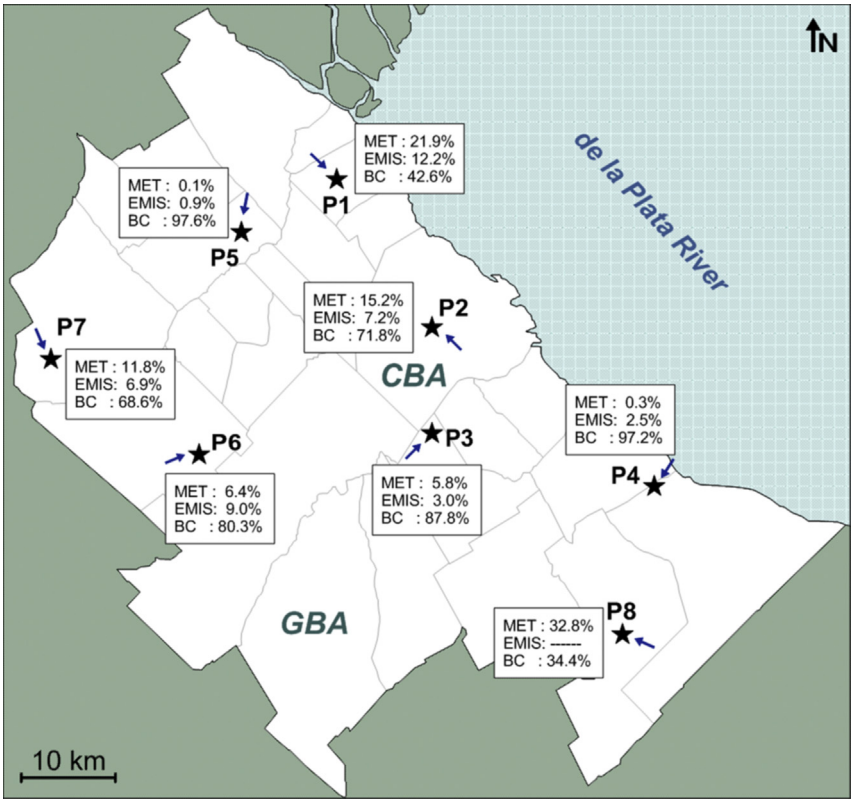

Fig. 3. Total variance explained (%) by each category of input variables (MET: atmospheric variables, EMIS: local emission rates of NO_x and VOC, BC: regional background ozone concentration) at eight selected receptor in the MABA (=CBA + GBA). Wind direction at the time of occurrence of C_{max}(BC) is indicated by the blue arrow. (For interpretation of the references to colour in this figure legend, the reader is referred to the web version of this article.)

which suggests a production of ozone compared to the regional level. A closer inspection at the GRS equations (Azzi et al., 1992) shows that a net production of ozone can occur when the ratio of the reaction constant of the NO_2 photolysis (k_3) to that of the O_3 titration (k_4) is maximum and/or the conversion of NO to NO_2 is maximum. Since the ratio k_3/k_4 increases with the solar radiation, it maximises around midday hours. Therefore, only a maximum ratio of NO_2/NO_x can explain a peak of O_3 at early morning or late evening hours. At suburban receptors, a larger conversion $NO \rightarrow NO_2$ is expected. This, combined with higher emission rates from upwind sources and greater atmospheric stability at these hours, may lead to enough NO_2 to generate some O_3.

3.2. The relative contributions of the input variables at selected receptors

Fig. 4 shows that the diurnal variation of the uncertainty of C_h (i.e., its 95% confidence interval) during the day of occurrence of C_{max}(BC) may differ considerably at different receptors. Among the eight selected receptors, the maximum-to-minimum diurnal ratio of the C_h uncertainty varies between 1.2 (P1) and 13.7 (P2) without an identifiable spatial pattern. The maximum uncertainty of C_h occurs mainly at 6–7 h or 19 h, when atmospheric photochemistry plays a minor role. Therefore, this uncertainty may probably result from errors related with the emissions and the physical module (DAUMOD) rather than with the chemical scheme (GRS). Results obtained by other authors for other urban areas using more complex models have some similarities. For example, Chen and Brune (2012) have also estimated a larger uncertainty at rush hours in the morning but mostly related to the chemistry. On the other hand, Rodriguez et al. (2007) have also found that the hours of largest uncertainty do not match those of peak ozone concentrations. The mean values of C_h at the time of occurrence of C_{max}(BC) (not shown) tend to those of Table 2 (i.e., they converge). The

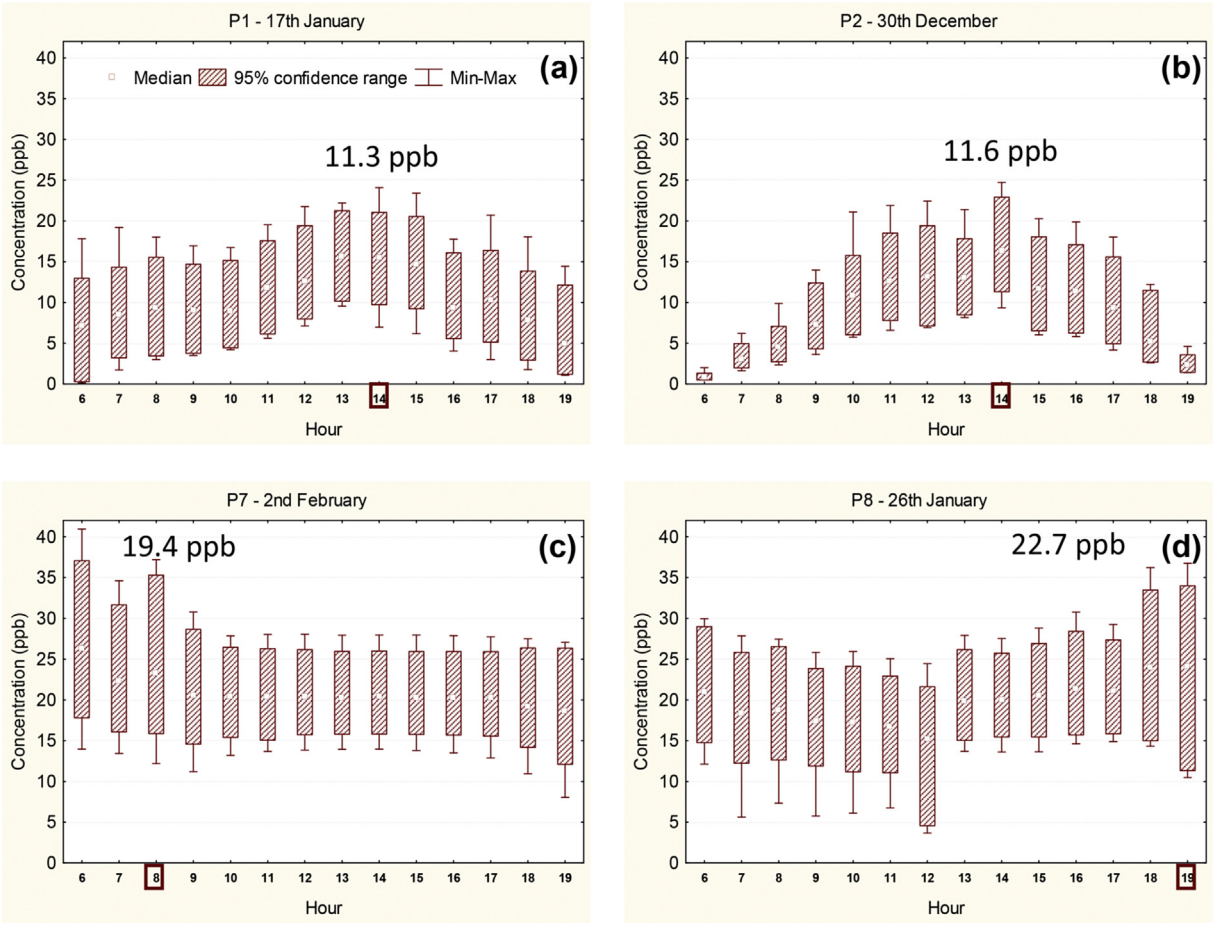

Fig. 4. Diurnal variation of the uncertainty (95% confidence range) of hourly O_3 concentrations (C_h) at receptors P1 (a), P2 (b), P7 (c) and P8 (d) during the day of occurrence of their corresponding C_{max}(BC) values. The times of occurrence and uncertainty values are indicated.

uncertainty of C_h at the hour of occurrence of C_{max}(BC) at these receptors varies between 10.6 and 22.7 ppb, which approximates quite well to their corresponding C_{max} uncertainty values (Fig. 2).

At each of the selected receptors shown in Fig. 3, the multiple linear regression analysis is applied using the set of C_h values obtained from the MC runs at the hour of occurrence of C_{max}(BC).

Considering the possible effects of the input variables on O_3 concentrations may be useful to anticipate what kind of correlations (positive or negative) can be expected. The complex nature of ozone makes its concentration behave differently under different environmental conditions (e.g., Clapp and Jenkin, 2001; Sillman and Samson, 1995). For example, wind speed (U) and atmospheric stability class (KST) only affect transport and dispersion of pollutants. Enhanced dispersion may result from a positive perturbation of U or a negative perturbation of KST, leading to more diluted precursor species concentrations, which in turn can increase or decrease O_3 levels depending on other environmental conditions. Air temperature (T), sky cover (SC) and total solar radiation (TSR) can affect both atmospheric dispersion and photochemistry. Increased T or TSR values, or decreased SC can favour any of the two processes; therefore, the correlations between these variables and C_h will also depend upon which processes are dominating. In the case of wind direction (DIR), the significance of its correlation will depend on the specific receptor (i.e., whether the site presents a homogeneous pollution rose or if it is located where an abrupt spatial change of emissions exists, like a costal site), and its sign will be determined by the distribution of emission sources around it. Emission rates of nitrogen oxides (QNO_x) and volatile organic compounds (QVOC) can also present positive or negative correlations with ozone hourly concentrations. For example, a positive correlation between O_3 and QNO_x is expected under a NO_x-limited regime (typical of rural areas); while a negative correlation can occur under a VOC-limited regime (commonly found in urban areas).

Tables 3 and 4 present the standardised multiple regression coefficients (β_i) of each input variable x_i and its uncertainty contribution (UC_i) to the total uncertainty of C_h at the hour of occurrence of C_{max}(BC), respectively. The sign of β_i determines if the correlation between x_i and C_h is positive or negative (correlations that are significant at the 95% level are indicated by bold numbers). As expected, the uncertainties of C_h at all receptors are found to be: positively correlated with uncertainties of $[O_3]_r$, under a VOC-limited regime and almost uncorrelated with uncertainties of local QVOC. On the other hand, no significant correlation is obtained between the uncertainties of C_h and those of T, SC, TSR which is consistent with the hypothesis of Bogo et al. (1999) who suggest that the urban atmosphere of Buenos Aires has a low oxidative capacity. At receptors with high emission rates (P1-P3), a positive β_U and a negative β_{KST} are obtained (i.e., increased O_3 levels are favoured by enhanced dispersion conditions). The opposite effect, but at a less significant level, is observed at suburban receptors (P6-P8). As hypothesised above, this difference could be due to the fact that C_{max} may be controlled by different reactions. In the first case, enhanced atmospheric dispersion reduces NO concentrations

Table 3
Standardised multiple regression coefficients (β_i) for the DAUMOD-GRS input variables (U: wind speed, DIR: wind direction, T: air temperature, SC: sky cover, KST: atmospheric stability class, TSR: total solar radiation, QNO_x: local NO_x emission rate, QVOC: local VOC emission rate, $[O_3]_r$: regional background O_3 concentration) at the selected receptors shown in Fig. 3. Bold numbers are significant at the 95% level.

Receptor	U	DIR	T	SC	KST	TSR	QNO_x	QVOC	$[O_3]_r$
P1	**0.292**	0.059	−0.081	−0.010	**−0.345**	0.067	**−0.348**	−0.032	**0.652**
P2	**0.103**	**0.093**	**0.073**	−0.016	**−0.356**	−0.015	**−0.261**	0.059	**0.847**
P3	0.044	**−0.053**	0.036	−0.005	**−0.228**	0.004	**−0.173**	0.021	**0.937**
P4	0.005	**−0.047**	−0.004	−0.007	0.028	0.010	**−0.159**	0.001	**0.986**
P5	−0.004	−0.019	−0.008	−0.004	0.001	0.009	**−0.095**	0.014	**0.988**
P6	**−0.082**	**−0.213**	0.010	0.031	**0.101**	−0.023	**−0.298**	−0.030	**0.896**
P7		**0.298**	0.007	0.031	**0.154**	−0.066	**−0.256**	−0.056	**0.828**
P8		**0.522**	0.012	−0.015	**0.225**	0.065			**0.586**

Table 4
Uncertainty contribution (%) of each input variable (UC_i) shown in Table 3. Bold numbers are significant at the 95% level.

Receptor	U	DIR	TA	SC	KST	TSR	QNO_x	QVOC	$[O_3]_r$
P1	**8.5**	0.4	0.7	0.0	**11.9**	0.5	**12.1**	0.1	**42.6**
P2	**1.1**	**0.9**	**0.5**	0.0	**12.7**	0.0	**6.8**	0.4	**71.8**
P3	0.2	**0.3**	0.1	0.0	**5.2**	0.0	**3.0**	0.0	**87.8**
P4	0.0	**0.2**	0.0	0.0	0.1	0.0	**2.5**	0.0	**97.2**
P5	0.0	0.0	0.0	0.0	0.0	0.0	**0.9**	0.0	**97.6**
P6	**0.7**	**4.5**	0.0	0.1	**1.0**	0.1	**8.9**	0.1	**80.3**
P7	–	**8.9**	0.0	0.1	**2.4**	0.4	**6.5**	0.3	**68.6**
P8	–	**27.3**	0.0	0.0	**5.1**	0.4	–	–	**34.4**

which in turn reduces O_3 tritation; while in the second, decreased dispersion increases NO_2 concentrations which increases those of O_3.

The relative contributions from the input variables vary spatially as shown in Table 4, with C_h uncertainties being dominated by uncertainties in different variables at different receptors, as also obtained in previous studies at other cities (e.g., Hanna et al., 1998; Kioutsiouski et al., 2005). The uncertainty contribution from the wind speed (UC_U) is usually low (<1%), except at receptor P1 (8.5%) which presents relatively high NO_x and VOC emission rates and wind speed at the time of occurrence of C_{max}(BC) (see Table 2). This higher UC_U value could be reflecting that C_h is more sensitive to U for higher wind speeds (regardless the emission conditions of the receptor), which would be probably more related to the physical module of the DAUMOD-GRS than to the chemical one; however, more numerical experiments are needed to confirm this hypothesis. On the other hand, the greatest UC_{DIR} values (up to 26.6%) occur near the boundary of the MABA. This is expected since in the present work, only the emissions from the MABA are considered and a small change of wind direction can lead to a large change in the emission sources that affect these receptors. UC_{QNOx} varies between 0.9 and 12.1% but no clear spatial pattern is observed.

Finally, by summing the UC_i values by category of input variable (atmospheric, emission and regional background concentration data), it is found that the uncertainty in regional background conditions dominates at all receptors (see Fig. 3). Its relative contribution varies considerably between 34.4 and 97.6%, being greater (>80%) at receptors of moderate NO_x and VOC emission rates (P3-P6). The uncertainty in the input meteorological data makes the second most important contribution (with more than 10%) to the C_h uncertainty at P1, P2, P7 and P8. At receptors of relatively high emission rates and wind speeds (P1 and P2), such contribution is dominated by the uncertainty contributions from U and KST (due to a greater sensitivity of C_h to atmospheric dispersion); while at receptors near the boundary of the MABA (P7 and P8), possible errors in DIR become more significant (as a consequence of a greater sensitivity of C_h to wind direction, as described above).

4. Conclusions

A methodology based on the Monte Carlo analysis is implemented to assess the uncertainty of 1-h peak O_3 concentrations at each receptor in the Metropolitan Area of Buenos Aires (MABA) during the summer (C_{max}) modelled with the DAUMOD-GRS due to uncertainties in the model input data. High resolution (1 km^2) spatial distributions of mean and uncertainty C_{max} values in the MABA are obtained. Mean C_{max} varies spatially between 15.3 and 50.9 ppb, while C_{max} uncertainty (taken as the 95% confidence interval) is in the range 9.3–47.0 ppb. Results show that the potentially high (>40 ppb) peak O_3 levels previously simulated for the surroundings of the MABA are subject to the greatest model uncertainty.

At different receptors of the MABA, the values of C_{max} obtained from the base case run [C_{max}(BC)] occur not only at different hours but also at different days of the summer. The diurnal variation of the uncertainty of the O_3 hourly concentration (C_h) during the day of occurrence of C_{max}(BC) varies considerably among eight selected receptors, showing that despite being a simple model, DAUMOD-GRS gives acceptable responses. Multiple linear regression analysis is applied at these receptors to evaluate the relative contributions of the input variables uncertainties to that of C_h at the time of occurrence of C_{max}(BC). The results obtained show that, although their relative contributions vary spatially, the uncertainty in the regional background ozone concentration dominates at all the analysed receptors, accounting for 34.4–97.6% of modelled concentration uncertainty. The meteorological input variables play a second role at receptors with high emission rates (where C_h is more sensitive to atmospheric dispersion) and at those near the boundary of the MABA (through a greater effect of wind direction). Therefore, the greatest uncertainties obtained for the greatest C_{max} values outside the MABA could be reduced by improving the estimations of the regional background O_3 concentrations. In the absence of ozone observations at rural monitoring stations upwind the MABA, the second most adequate approach to improve such estimations would be using a larger scale air quality model which allows the evaluation of the contribution from remote emission sources.

Acknowledgements

Professor Laura E. Venegas has recently passed away. Laura was an outstanding scientist who had the ability to transform complex concepts or ideas into simpler ones. Her deep knowledge on the subject combined with her enthusiasm, generosity, commitment and extremely positive attitude towards scientific work, have been a source of inspiration for those of us who had the enormous privilege to share our lives with her. Laura will live in our memories as the exceptional human being she was.

The authors thank the two anonymous reviewers for their

comments and suggestions which greatly contributed to improve this work. This study has been supported by CONICET Project PIP0304.

References

Athanassiadou, M., Baker, J., Carruthers, D., Collins, W., Girnary, S., Hassell, D., Hort, M., Johnson, C., Johnson, K., Jones, R., Thomson, D., Trought, N., Witham, C., 2010. An assessment of the impact of climate change on air quality at two UK sites. Atmos. Environ. 44, 1877–1886.

Azzi, M., Johnson, G., Cope, M., 1992. An introduction to the generic reaction set photochemical smog model. In: Proc. 11th Int. Clean. Air Conf., pp. 451–462.

Borrego, C., Monteiro, A., Ferreira, J., Miranda, A.I., Costa, A.M., Carvalho, A.C., Lopes, M., 2008. Procedures for estimation of modelling uncertainty in air quality assessment. Environ. Int. 34, 613–620.

Bergin, M.S., Noblet, G.S., Petrini, K., Dhieux, J.R., Milford, J.B., Harley, R.A., 1999. Formal uncertainty analysis of a Lagrangian photochemical air pollution model. Environ. Sci. Technol. 33, 1116–1126.

Bogo, H., Negri, R.M., San Román, E., 1999. Continuous measurement of gaseous pollutants in Buenos Aires city. Atmos. Environ. 33, 2587–2598.

Calfapietra, C., Fares, S., Manes, F., Morani, A., Sgrigna, G., Loreto, F., 2013. Role of Biogenic Volatile Organic Compounds (BVOC) emitted by urban trees on ozone concentration in cities: a review. Environ. Pollut. 183, 71–80.

Chang, J.C., Hanna, S.R., 2005. Technical Descriptions and User's Guide for the BOOT Statistical Model Evaluation Software Package, Version 2.0, p. 64. Available on. http://www.harmo.org/Kit/Download/BOOT_UG.pdf.

Chen, S., Brune, W., 2012. Global sensitivity analysis of ozone production and O_3-NO_x-VOC limitation based on field data. Atmos. Environ. 55, 288–296.

Clapp, L.J., Jenkin, M.E., 2001. Analysis of the relationship between ambient levels of O_3, NO_2 and NO as a function of NO_x in UK. Atmos. Environ. 35, 6391–6405.

Derwent, D., Fraser, A., Abbott, J., Jenkin, M., Willis, P., Murrells, T., 2010. Evaluating the Performance of Air Quality Models. DEFRA Report. Issue 3/June 2010. Available on. http://www.airquality.co.uk/reports/cat05/1006241607_100608_MIP_Final_Version.pdf.

Derwent, R.G., Murrells, T.P., 2013. Impact of policy-relevant scenarios on ozone in southern England: influence of chemical mechanism choice. Atmos. Environ. 72, 89–96.

Dunker, A.M., Yarwood, G., Ortmann, P., Wilson, G.M., 2002. The decoupled direct method for sensitivity analysis in a three-dimensional air quality model - implementation, accuracy, and efficiency. Environ. Sci. Technol. 36, 2965–2976.

Hanna, S.R., Chang, J.C., Fernau, M.E., 1998. Monte Carlo estimates of uncertainties in predictions by a photochemical grid model (UAM-IV) due to uncertainties in input variables. Atmos. Environ. 32 (21), 3619–3628.

Hanna, S.R., Paine, R., Heinold, D., Kintigh, E., Baker, D., 2007. Uncertainties in air toxics calculated by the dispersion models AERMOD and ISCST3 in the houston ship channel area. J. Appl. Meteorol. Climatol. 46, 1372–1382.

Hanna, S.R., Russell, A.G., Wilkinson, J.G., Vukovich, J., Hansen, D.A., 2005. Monte Carlo estimation of uncertainties in BEIS3 emission outputs and their effects on uncertainties in chemical transport model predictions. J. Geophys. Res. 110, D01302. http://dx.doi.org/10.1029/2004JD004986.

Hurley, P.J., Physick, W.L., Luhar, A.K., 2005. TAPM: a practical approach to prognostic meteorological and air pollution modelling. Environ. Model. Softw. 20, 737–752.

Kim, C.-H., Park, S.-U., Song, C.-K., 2005. A simple semi-empirical photochemical model for the simulation of ozone concentration in the Seoul metropolitan area in Korea. Atmos. Environ. 39, 5597–5607.

Kioutsioukis, I., Melas, D., Zerefos, C., Ziomas, I., 2005. Efficient sensitivity computations in 3D air quality models. Comput. Phys. Commun. 167, 23–33.

Lee, Y.C., Shindell, D.T., Faluvegi, G., Wenig, M., Lam, Y.F., Ning, Z., Hao, S., Lai, C.S., 2014. Increase of ozone concentrations, its temperature sensitivity and the precursor factor in South China. Tellus B 66, 23455. http://dx.doi.org/10.3402/tellusb.v66.23455.

Mazzeo, N.A., Venegas, L.E., 1991. Air pollution model for an urban area. Atmos. Res. 26, 165–179.

Mazzeo, N.A., Venegas, L.E., 2008. Design of an air-quality surveillance system for Buenos Aires city integrated by a NO_x monitoring network and atmospheric dispersion models. Environ. Model. Assess. 13, 349–356.

Mazzeo, N.A., Venegas, L.E., Choren, H., 2005. Analysis of NO, NO_2, O_3 and NO_x concentrations measured at a green area of Buenos Aires City during winter-time. Atmos. Environ. 39, 3055–3068.

Moore, G.E., Londergan, R.J., 2001. Sampled Monte Carlo uncertainty analysis for photochemical grid models. Atmos. Environ. 35, 4863–4876.

Paoletti, E., Manning, W.J., 2007. Toward a biologically significant and usable standard for ozone that will also protect plants. A Review. Environ. Pollut. 150, 85–95.

Paoletti, E., De Marco, A., Beddows, D., Harrison, R., Manning, W.J., 2014. Ozone levels in European and USA cities are increasing more than at rural sites, while peak values are decreasing. Environ. Pollut. 192, 295–299.

Pineda Rojas, A.L., 2014. Simple atmospheric dispersion model to estimate hourly ground-level nitrogen dioxide and ozone concentrations at urban scale. Environ. Model. Softw. 59, 127–134.

Pineda Rojas, A.L., Venegas, L.E., 2009. Atmospheric deposition of nitrogen emitted in the metropolitan area of Buenos Aires to coastal waters of de la Plata River. Atmos. Environ. 43, 1339–1348.

Pineda Rojas, A.L., Venegas, L.E., 2013a. Upgrade of the DAUMOD atmospheric dispersion model to estimate urban background NO_2 concentrations. Atmos. Res. 120–121, 147–154.

Pineda Rojas, A.L., Venegas, L.E., 2013b. Spatial distribution of ground-level urban background O_3 concentrations in the Metropolitan Area of Buenos Aires, Argentina. Environ. Pollut. 183, 159–165.

Refsgaard, J.C., van der Sluijs, J.P., Højberg, A.L., Vanrolleghem, P.A., 2007. Uncertainty in the environmental modelling process e A framework and guidance. Environ. Model. Softw. 22, 1543–1556.

Rodriguez, M.A., Bouwer, J., Samuelsen, G.S., Dabdub, D., 2007. Air quality impacts of distributed power generation in the South Coast Air Basin of California 2: model uncertainty and sensitivity analysis. Atmos. Environ. 41, 5618–5635.

Russell, A., Dennis, R., 2000. NARSTO critical review of photochemical models and modelling. Atmos. Environ. 34 (12–14), 2283–2324.

Sillman, S., Samson, P.J., 1995. Impact of temperature on oxidant photochemistry in urban, polluted rural and remote environment. J. Geophys. Res. 100, 11497–11508.

Strong, J., Whyatt, J.D., Metcalfe, S.E., Derwent, R.G., Hewitt, C.N., 2013. Investigating the impacts of anthropogenic and biogenic VOC emissions and elevated temperatures during the 2003 ozone episode in the Uk. Atmos. Environ. 74, 393–401.

Tan, Y., Robinson, A.L., Presto, A.A., 2014. Quantifying uncertainties in pollutant mapping studies using the Monte Carlo method. Atmos. Environ. 99, 333–340.

Tang, X., Wang, Z., Zhu, J., Gbaguidi, A.E., Wu, Q., Li, J., Zhu, T., 2010. Sensitivity of ozone to precursor emissions in urban Beijing with a Monte Carlo scheme. Atmos. Environ. 44, 3833–3842.

Venegas, L.E., Mazzeo, N.A., 2006. Modelling of urban background pollution in Buenos Aires city (Argentina). Environ. Model. Softw. 21 (4), 577–586.

Venegas, L.E., Mazzeo, N.A., Pineda Rojas, A.L., 2011. Chapter 14: evaluation of an emission inventory and air pollution in the metropolitan area of Buenos Aires. In: Popovic, D. (Ed.), Air Quality-models and Applications, Editorial In-tech, pp. 261–288.

Venkatram, A., Karamchandani, P., Pai, P., Goldstein, R., 1994. The development and application of a simplified ozone modelling system (SOMS). Atmos. Environ. 28 (22), 3665–3678.

Wang, Y., Konopka, P., Liu, Y., Chen, H., Müller, R., Plöger, F., Riese, M., Cai, Z., Lü, D., 2012. Tropospheric ozone trend over Beijing from 2002–2010: ozonesonde measurements and modeling analysis. Atmos. Chem. Phys. 12, 8389–8399.

WHO, 2014. World Health Organization Media Centre, Air Quality and Health, Fact Sheet N.313. Updated March 2014 available online on. http://www.who.int/mediacentre/factsheets/fs313/es/.